3D MAGNETIC RECONNECTION AT AN X-RAY BRIGHT POINT

C. H. MANDRINI*
Instituto de Astronomía y Física del Espacio, IAFE-CONICET, CC.67, Suc. 28, 1428 Buenos Aires, Argentina

P. DÉMOULIN, L. VAN DRIEL-GESZTELYI** and B. SCHMIEDER
Observatoire de Paris, Section de Meudon, DASOP, URA 2080 (CNRS) F-92195 Meudon Cedex, France

G. CAUZZI***
Institute for Astronomy, University of Hawaii, Honolulu, HI 96822, U.S.A.

A. HOFMANN
Astrophysikaliches Institut Potsdam, Sonnenobservatorium Einsteinturn, D-14473 Potsdam, Germany

(Received 6 February, 1996; in final form 23 May, 1996)

Abstract. On May 1, 1993, a flaring X-ray bright point (XBP) was observed for about 16 hours in the old, disintegrating, bipolar active region (AR) NOAA 7493. During this period, a minor magnetic bipole (10^{20} Mx) emerged in the region. We have found observational evidence showing that the XBP brightenings were due to magnetic reconnection between the new bipole and pre-existing plage fields. The aim of the present work is to substantiate with magnetic modelling what has been shown by the observations. For this purpose we extrapolate the observed photospheric magnetic fields in the linear force-free approximation and follow its evolution during the lifetime of the XBP. From the computed coronal field lines we determine the location of regions of drastic change in field-line linkage, called 'quasi-separatrix layers' or QSLs. QSLs are open layers that behave physically like separatrices: the break down of ideal magnetohydrodynamics and the release of free magnetic energy may occur at these locations when their thickness is small enough. The extrapolated field lines, with photospheric footpoints on both sides of QSLs, match the observed chromospheric and coronal structures (arch filament system, XBP and faint X-ray loops (FXL)). We study also the evolution of the width of the QSL located over the new negative polarity pore: the calculated QSL is very thin (typically less than 100 m) during the lifetime of the XBP, but becomes much thicker ($\geq 10^4$ m) after the XBP has faded. Furthermore we show that peaks in X-ray brightness propagate along the FXL with a velocity of ≈ 670 km s^{-1}, starting from the XBP location, implying that the energy is released where the emerging bipole impacts against pre-existing coronal loops. We discuss the possible mechanism of energy transport and conclude that the energy is conducted to the remote footpoints of the FXL by a thermal front. These results strongly support the supposition that the XBP brightness and flaring are due to the interaction of different flux systems, through 3D magnetic reconnection, at QSLs.

1. Introduction

X-ray bright points (XBPs) were first observed in images obtained by a rocket-borne grazing-incidence soft X-ray telescope (van Speybrock, Krieger, and Vaiana, 1970) and their characteristics were analysed in detail during the *Skylab* mission

* Member of the Carrera del Investigador Científico, CONICET.
** Also at Konkoly Observatory, Budapest, Pf. 67, H-1525 Hungary.
*** Present address: Osservatorio Astronomico di Capodimonte, Napoli, Italy.

Solar Physics **168:** 115–133, 1996.

(Golub *et al.*, 1974, 1977; Golub, Krieger, and Vaiana, 1976). They appear as diffuse clouds of typically 20 Mm diameter with a central bright core. They are uniformly distributed over the solar surface, with about 200 being present simultaneously and 1500 being born each day. Their lifetimes vary between 2 and 48 hours, with a mean value of 8 hours, and they are located above pairs of opposite polarity flux features observed in the photosphere (Harvey, 1993; Harvey *et al.*, 1994). Golub *et al.* (1974) first pointed out the occurrence of flares in XBPs. Nolte, Solodyna, and Gerassimenko (1979) observed impulsive brightenings and rapid decays in a small sample of XBPs. They suggested that the fluctuations were driven by episodic heating superimposed upon a continuous input of energy. The cause of XBP variability is not yet clear, although recent results indicate that the XBP brightenings are similar to normal flares, only smaller in energy (e.g., Strong *et al.*, 1992), and with even the presence of nonthermal acceleration of particles (Kundu *et al.*, 1994).

Based on *Skylab* results, XBPs were originally considered the primary coronal manifestation of emerging photospheric flux. However, subsequent studies gave contradictory results concerning the nature of XBPs. Martin *et al.* (1985) suggested that cancelling features could be associated with XBPs, provided that they are more numerous than and similar in scale to ephemeral ARs and that it is unlikely that there are enough ephemeral regions to account for all XBPs. On the other hand, Golub, Harvey, and Webb (1986) found that XBPs are more likely associated with emerging than with cancelling flux. More recently Webb *et al.* (1993), analyzing X-ray data from rocket flights coordinated with full-disk and time-lapse magnetograms on two different days, reached the conclusion that two-thirds of XBPs lie above decaying or cancelling magnetic features. Apart from the controversy, the important point to draw from these results is that the appearance of an XBP in the corona is independent of the type of feature seen in the magnetogram, as long as it is a bipole. In the previous scenarios, XBPs imply the interaction of different flux systems via coronal magnetic reconnection, either driven by the emergence of the new magnetic flux against the overlying coronal field or driven by the approach of opposite magnetic features that can eventually cancel afterwards.

In this paper we will deal with a flaring XBP observed on May 1, 1993 in the decaying AR 7493 (S11, central meridian passage on May 3, 1993). The detailed analysis of the ground-based optical observations coordinated with X-ray data from the Soft X-ray Telescope (SXT, Tsuneta *et al.*, 1991) aboard *Yohkoh* has been presented in van Driel-Gesztelyi *et al.* (1996), hereafter Paper I. This XBP appeared to be related to a new emerging minor bipole of about 10^{20} Mx. Its sudden enhancements and global soft X-ray light curve were interpreted as due to magnetic reconnection between the new bipole and the pre-existing plage fields.

The 3D characteristics of magnetic reconnection are highly complex, and it is not evident that the properties of 2D and $2\frac{1}{2}$D models can be extended to 3D (Schindler, Hesse, and Birn, 1988; Priest and Forbes, 1992; Lau and Finn, 1990; Priest and Titov, 1996). Only for cases where magnetic null points or field lines

tangent to the photosphere are present in the configuration, is it possible to identify separatrix surfaces (see, e.g., Lau, 1993; Bungey, Titov, and Priest, 1996). The separatrices divide up the magnetic volume into topologically distinct regions, that is to say, the field-line linkage is discontinuous across these surfaces that intersect at the separator. When reconnection occurs, magnetic flux is transferred across the separatrices from one region to another. Following this line, several studies (Gorbachev and Somov, 1988, 1989; Mandrini *et al.*, 1991, 1993, 1995; Démoulin *et al.*, 1993, 1994; van Driel-Gesztelyi *et al.*, 1994; Bagalá *et al.*, 1995) have related the location of flare brightenings to the topology deduced from the observed photospheric field modeled by subphotospheric magnetic sources. The topology has been defined by the magnetic link between these sources. Recently, Priest and Démoulin (1995) have generalized the concept of separatrices to configurations without field-line linkage discontinuities. They propose that magnetic reconnection may occur in 3D in the absence of null points at 'quasi-separatrix layers' (QSLs), which are regions where there is a steep gradient or a drastic change in the mapping of field lines from one boundary to another of a given magnetic volume. They analyse a sheared X-field where nearly any smooth and weak flow imposed on the boundary produces strong flows at the QSLs. Démoulin *et al.* (1996a) have determined the location of QSLs and studied their properties in simple theoretical flaring configurations built by four magnetic sources. For this purpose they have developed a numerical algorithm called QSLM, for the 'quasi-separatrix' layers method.

So as to test quantitatively the results of Paper I, in this paper we apply the QSLM to AR 7493. In Section 2 we summarize the observations that are relevant to this study. After briefly describing the QSLM, we study in Section 3 the topological evolution of AR 7493, add more observational evidence in favour of the nature of this XBP as a reconnected loop, and discuss our results. In the final section we conclude on the characteristics of energy release in this XBP.

2. Summary of the Observations

Ground-based data coordinated with *Yohkoh*/SXT observations of AR 7493 provided a multiwavelength (magnetic field, Hα and X-ray) data base for the study of a flaring 'active region' XBP, of about 16 hour lifetime, and of the activity related to it in different layers of the solar atmosphere. The XBP became visible in the solar corona on May 1 at about 04:00 UT and disappeared after 21:00 UT on the same day (see Figure 1). The XBP appeared to be related to a new minor bipole of about 10^{20} Mx. In the chromosphere, an arch filament system (AFS) was observed connecting the opposite polarity parts of the new bipole. The XBP was located near this new flux emergence, but not above it. In fact it appeared to be between the negative-polarity new field and a pre-existing positive polarity plage field (see Section 3.5). The XBP shifted during its existence following the negative

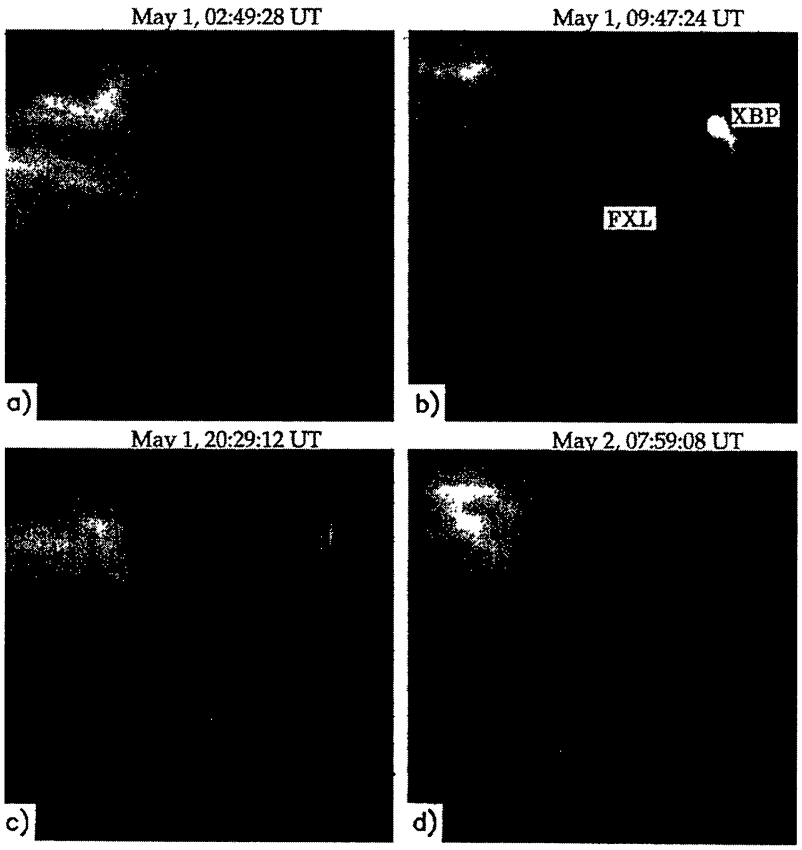

Figure 1. SXT images of AR 7493: (a) before, (b, c) during, and (d) after the presence of the XBP. The continous lines in Figure1(c) delimit the borders of the magnetogram shown in Figure 2 (while the computations are done using the full magnetogram).

polarity new field, which was moving with a velocity of about 0.2 km s^{-1} around the pre-existing plage. The XBP shifted so that it always remained between the new and the pre-existing fields.

Superimposed on a global evolution of soft X-ray brightness, the XBP displayed sudden enhancements lasting for 1 to 10 min (see Figure 6 and Table 3 in Paper I). During these brightenings the XBP apparently had a spatial structure that was (tiny) loop-like rather than point-like (Figure 1(b)). The tiny loop was oriented so that it connected the new and pre-existing fields, suggesting that the XBP represented a hot coronal loop between them. Such connection, as shown here, could only be established through magnetic field line reconnection. Some heating, temporally coincident with the XBP brightenings, occurred along related faint X-ray loops (denoted FXL, see Figures 1(b) and 1(c)). Brightness enhancements of the remote footpoints (see Section 3.5) were found suggesting that the loops were heated by both fast particles and a conduction front.

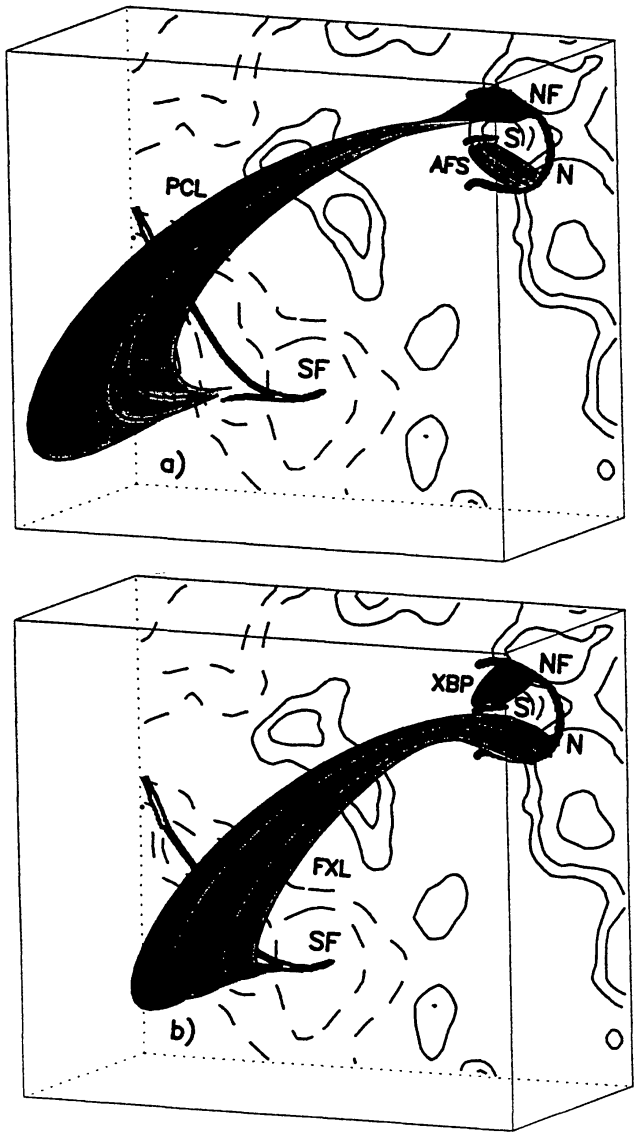

Figure 2. Extrapolated coronal field lines related to the observed chromospheric and coronal features and the photospheric location of the QSLs superimposed on the H2 magnetogram (22:45 UT). The QSLs are indicated by the thick isocontour of $N = 20$ at the photospheric level. The four sets of computed field lines (drawn with surfaces) have their footpoints along the borders of the QSLs. In (a) the emerging flux, observed as an arch filament system (AFS), impacts against the pre-existing coronal loops (PCL). In (b) the reconnected field-lines appear as the X-ray bright point (XBP) and the faint X-ray loops (FXL). In this 3D view the box axes are parallel to the local x, y, and z coordinates, heliographic W and N are to the right (in x) and up (in y), respectively. The isocontour levels of B_l (longitudinal magnetic field) are ± 40, 100, and 400 G, with positive and negative values drawn with solid and dashed lines, respectively. The related photospheric flux concentrations are denoted by the letters N, NF, S, and SF, indicating their polarities, as in Paper I (see text).

3. The XBP in the Context of 3D Magnetic Reconnection

3.1. Brief Description of the Quasi-Separatrix Layers Method

The QSLM and the properties of QSLs have been discussed in detail by Démoulin *et al.* (1996a), so we address here only those aspects related to the results obtained

for AR 7493. The method is based in finding the location of QSLs on a given plane. These are regions where a drastic change in field-line linkage occurs. QSLs are defined in terms of a function that we call N, following Priest and Démoulin (1995). If we integrate a field line passing at a point $P(x, y, z)$ of the corona over a distance s in both directions, the points (x', y', z') and (x'', y'', z''), coordinates of the two end points, define a vector $\mathbf{D}(x, y, z) = \{X_1, X_2, X_3\} = \{x'' - x', y'' - y', z'' - z'\}$. A drastic change in field-line linkage means that for a slight shift of point $P(x, y, z)$, $\mathbf{D}(x, y, z)$ varies greatly. In the solar case, the distance s to be used is the distance to the photosphere ($z' = z'' = 0$) and the expression for $N(x, y)$ is

$$N(x, y) = \sqrt{\sum_{i=1,2} \left[\left(\frac{\partial X_i}{\partial x} \right)^2 + \left(\frac{\partial X_i}{\partial y} \right)^2 \right]}. \tag{1}$$

This function represents the norm of the displacement gradient tensor defined when mapping, by field lines, points on one boundary to the other of a given magnetic volume; both boundaries correspond to different sections of the photosphere in our particular case. The locations of the high values of $N(x, y)$ characterize the field lines involved in the QSLs; following these lines we can locate the coronal parts of these layers. QSLs are layers behaving physically like separatrices when their thickness is small enough so that the resistive term in the induction equation is important for the magnetic field evolution. The QSLM has been applied (Démoulin *et al.*, 1996b) to observed flaring ARs presenting different magnetic configurations, from quadrupolar to bipolar ones and from nearly potential to sheared ones. This is the first time in which we deal with a minor energetic event such as an XBP occurring in a decaying region.

3.2. Relationship between the observed features and the extrapolated field lines

The observed longitudinal field of AR 7493 is extrapolated to the corona using the discrete fast Fourier transform method under the linear force-free hypothesis ($\nabla \times \mathbf{B} = \alpha \mathbf{B}$), as proposed by Alissandrakis (1981). As the AR studied is slightly away from the solar-disk centre, we use a transformation of coordinates from the observed frame to the local one. This technique has been discussed by Démoulin *et al.* (1996b).

The evolution of the observed magnetic field in AR 7493 has been discussed in detail in Paper I and summarized in Section 2. Since in this paper we will not show the observed data, but only the results of our extrapolation, we refer the reader to that paper. In Paper I, Figure 2 displays the global magnetic configuration of AR 7493 over three days (April 30, May 1, and May 2, 1993), while Figure 3 shows in detail the magnetic evolution of the new emerging flux on the day it was first observed (May 1). We have selected four magnetograms from the dataset analysed in Paper I for our topological study. These magnetograms, which span

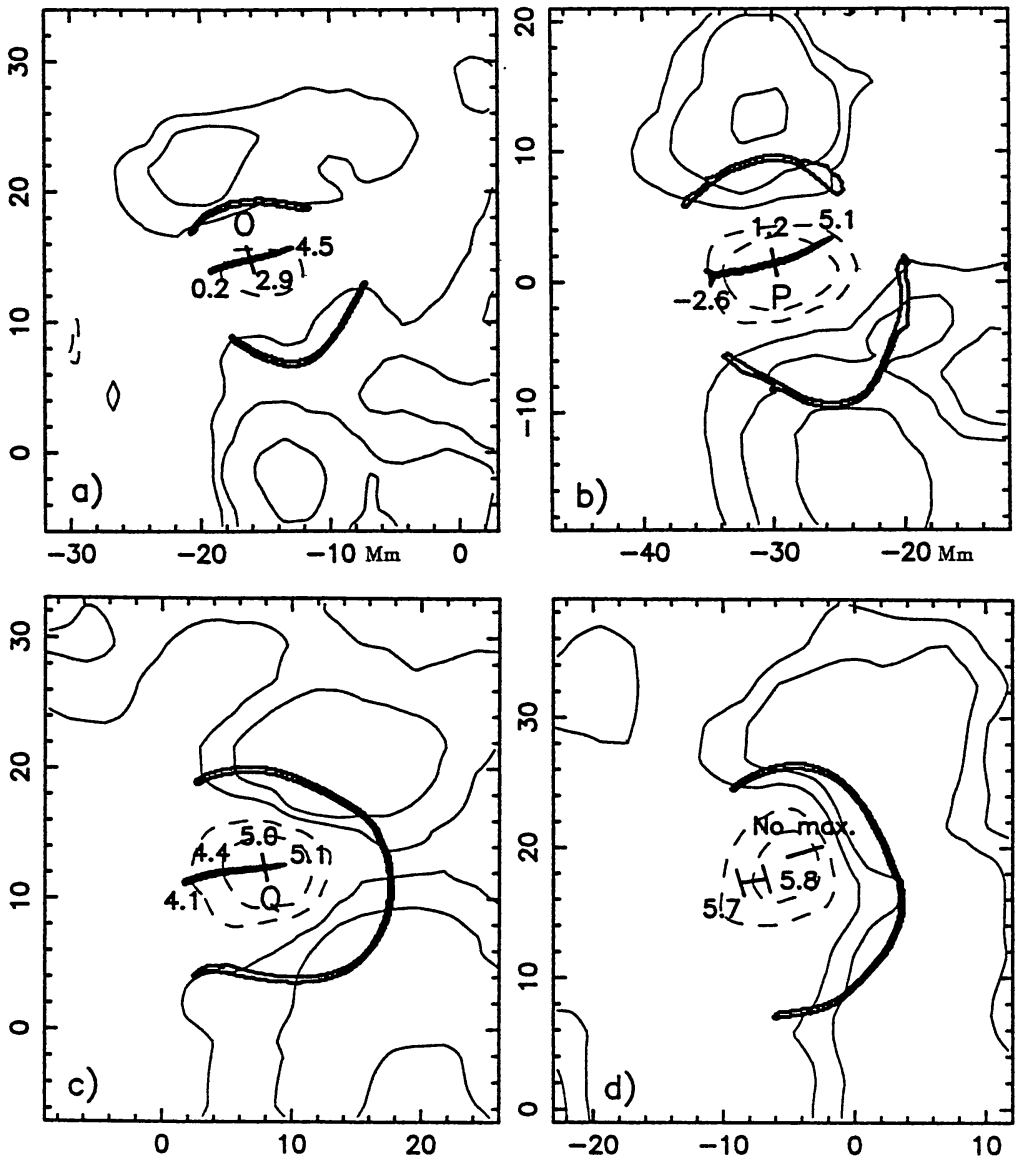

Figure 3. Spatial evolution of the QSLs as the new magnetic flux grows and moves (partial field of view of Figure 2). (a)–(d) correspond to P1 (07:16 UT), H1 (16:26 UT), H2 (22:45 UT), and P2 (08:02 UT) magnetograms, respectively. The axes are parallel to the local x and y coordinates. Isocontours of B_z (vertical field component) and of N have been drawn with the same values as those used in Figure 2. O, P, and Q show the positions where functions N, D, L, and T are analysed (see Figure 4 and text). The decimal logarithm of the QSL thickness (in m) is added at some characteristic places along the central QSL.

the full XBP lifetime, have been obtained with the Stokes polarimeter at Mees Solar Observatory, Hawaii (Mickey, 1985), and with the vector magnetograph in Potsdam (Staude *et al.*, 1991). Three of them correspond to May 1 at 07:16 UT (P1), 16:26 UT (H1), 22:45 UT (H2) and the last one to May 2 at 08:02 UT (P2). The letters H and P have been used to identify the magnetic data from Hawaii or Potsdam, respectively.

Figure 2 shows the extrapolated magnetic field and the location of QSLs at photospheric level for the H2 magnetogram. We show in these and the next figures only those QSLs that are (in H1 and P1 magnetograms) or were (in H2 and P2 magnetograms) located in the vicinity of the loops involved in the event. Although the transverse field measurements from Hawaii and Potsdam are rather noisy in this low-field region, photospheric shear is observed in the old, negative, field concentration, SF, and in the old, positive, field concentration to the south of polarity N. In this zone, the direction of the observed transverse component, of the field forms an average angle of 30° with the direction of the extrapolated photospheric transverse component, assuming a potential field. Also, at coronal heights, the existence of magnetic shear is suggested by the direction of the FXL observed in SXT images, as compared with that of the extrapolated coronal lines in the potential approach. We have found that a value of $\alpha \approx 0.02\ \mathrm{Mm}^{-1}$ is the best to fit the observations.

In what follows we have used the same letters as in Paper I to identify the different flux concentrations, except for the south positive polarity, where B has been replaced by SF for consistency. In Figure 2 four sets of field lines issued from the edges of QSLs are shown for the extrapolated field with $\alpha \approx 0.02\ \mathrm{Mm}^{-1}$. Each set defines a flat ribbon that is drawn as a surface. How can we relate these extrapolated field lines to the observations? Since we have only few magnetograms, we cannot model a time evolution of the region; we rather use the same magnetogram (H2) to determine the magnetic field lines implied both before and after reconnection. This is possible because the reconnection time of individual loops is much shorter than the global evolution time, so that the vertical photospheric field component does not change significantly during the process. Moreover, because QSLs are very thin (as shown below), a very slight change in the coronal electric currents can bring, after reconnection, magnetic field lines from one QSL side to the other. These properties allow us to interpret the sets of field lines as corresponding to a time before (Figure 2(a)) and after (Figure 2(b)) magnetic reconnection. Field lines linking N to S correspond to the AFS observed in Hα. As the new flux emerges and S shifts towards NF, the associated loops impact against the pre-existing coronal loops (PCL), that is, field lines joining NF to SF. The reconnected loops resulting from this interaction correspond to field lines joining NF to S, the observed XBP, and N to SF, the FXL observed in soft X-rays (compare Figures 1 and 2). Both sets of long loops, those before and after reconnection, link the positive flux concentrations (NF and N) to the negative flux at the south. Field lines involved in reconnection are found at both sides of QSLs as expected in a 3D reconnection process (Priest and Démoulin, 1995).

3.3. Topological evolution of AR 7493

The evolution of the QSLs associated with the emerging loops and the XBP loops is illustrated in Figure 3. These correspond to a partial view of AR 7493 centered

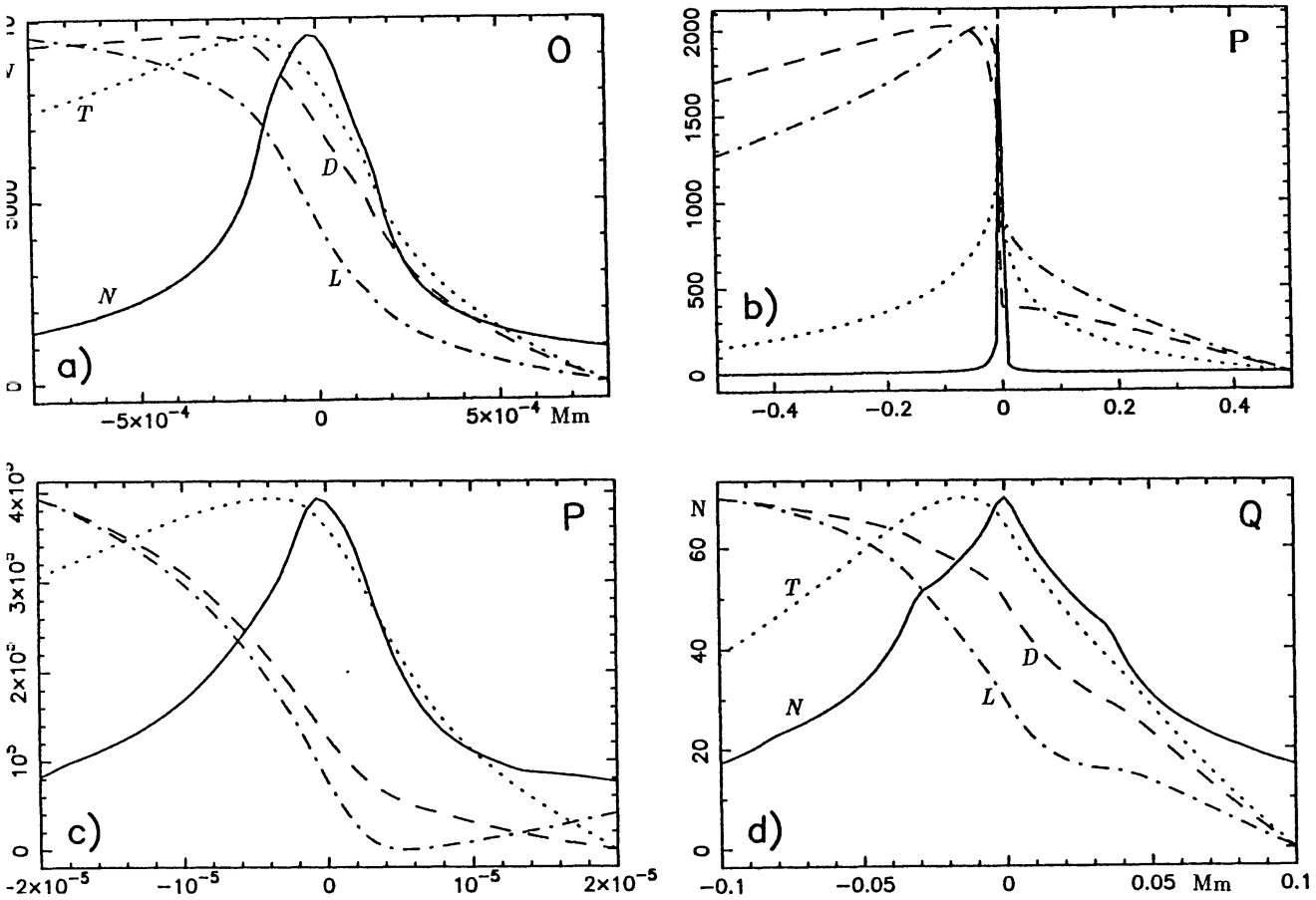

Figure 4. Evolution of the QSL located over the emerging negative polarity. The curves plotted are the distance D between the field-line footpoints (dashed curve), the field-line length L (dash-dotted curve), the delay function $T = \int ds/B$ (dotted curve) and the norm N (full lines) as functions of the abscissa of the initial field-line footpoint (see text). They have been obtained by cutting the QSL with a segment orthogonal to the QSL at points indicated in Figure 3: (a) at point O in P1 magnetogram; (b) and (c) at point P in H1 magnetogram (note that (b) has a larger scale range while (c) is a zoom view), and (d) at point Q in H2 magnetogram. The functions D, L, and T have been normalized to their minimum and maximum values in the range of the abscissa considered, while the labels of the vertical axis refer to the values of N.

on S and we are showing the same isocontour value ($N = 20$) as in Figure 2. It can be seen that the layer extending over S appears in all three magnetograms obtained on May 1. At the time of the P1 and H1 magnetograms, the XBP was visible, while it has already started fading in the *Yohkoh* images before the time of the H2 magnetogram (see Figure 6 in Paper I). On the other hand, no isocontour of $N = 20$ is present in this region on May 2. This shows that the QSL over S becomes less important (in the way quantified below) as S moves away from NF and N, which explains why the XBP faded on the evening of May 1.

Inside the isocontour of $N = 20$, shown in Figure 3, the function N takes much higher values in very thin and elongated regions. It is too expensive to resolve the variations of N numerically on the whole photospheric plane and it might be misleading to show the results on a 2D drawing (as in Figure 3) because the thicknesses of these elongated regions are much smaller than the

width of the line in the drawings. That is why we determine the behaviour of the function N cutting the QSLs with a segment at some localized points. Figure 4 depicts the changes in N along a segment orthogonal to the QSL on S at points O (Figure 4(a)), P (Figures 4(b) and 4(c)), and Q (Figure 4(d)); these are located where the photospheric magnetic field is highest (see Figure 3). The local shape of the function N remains basically the same as can be seen in Figure 4, the main difference being the scaling of the axes that changes by orders of magnitude. The thickness, δ, of the QSL defined as the width of the function N at half-height is inversely proportional to the maximum of the function N, $N_{\max}$; that is to say, $\delta \approx 5 \times 10^6/N_{\max}$ (in m). The values of the decimal logarithm of the thickness at different points along the QSL are shown in Figure 3. The QSL thickness is $\approx$ 800 m at O, 16 m at P and 9×10^4 m at Q. In P2 magnetogram, obtained on May 2, the function N shows no maximum along the central and western part of S; while along its eastern portion the QSL is very thick, $\approx 5 \times 10^5$ m.

The finding of these very thin structures in a magnetogram with 2 Mm resolution may look strange at first sight, but it is worth noticing that this does not mean having a numerical super-resolution! The thickness of QSLs is a global property of the magnetic configuration derived from field-line linkage. For example, in the particular case of a magnetic null point in the extrapolated coronal field, regardless of the resolution of the photospheric magnetogram, infinitely thin QSLs are present (in this case QSLs are separatrices). Then, there is no spurious problem in finding a QSL thickness much lower than the magnetogram resolution. The characteristics of QSLs are subjected to the same limitations as the magnetic field extrapolation: both require a well calibrated and resolved photospheric field. However, the thickness of QSLs increases rapidly with the size of photospheric field concentration; so, if there are unresolved magnetic features in the magnetogram, the QSLs thickness can be overestimated (see Démoulin *et al.*, 1996b, for a further discussion). Then the above values of the thickness are only upper bounds of the real ones.

Let us compare the evolution of the QSL thickness to the overall evolution of the XBP brightness (Figure 6 of Paper I). At the time of the first magnetogram P1 (May 1, 07:16 UT), the QSL was thin and the XBP had just started to brighten. Later the QSL became thinner and the intensity in X-rays increased. Unfortunately the next magnetogram (H1) corresponds to the decaying phase of the XBP, but the QSL thickness was still two orders of magnitude lower than in P1. As time went on, the QSL became thicker (the thickness is larger than 10^4 m in H2) and it even disappeared in P2 while the XBP faded. The XBP is observed for the last time at 21:00 UT on May 1 (when a five hour gap in the *Yohkoh* observation starts), this is 1 h 45 min before H2 magnetogram (see Paper I). This shows that there exists a relationship between the evolution of the QSL thickness and the XBP brightness. This result is interpreted in Section 3.4.

In the understanding of 3D magnetic reconnection other functions may have a theoretical interest (see Démoulin *et al.*, 1996a, for further comments). These are: the distance (D) between the photospheric footpoints of field lines, the field-line

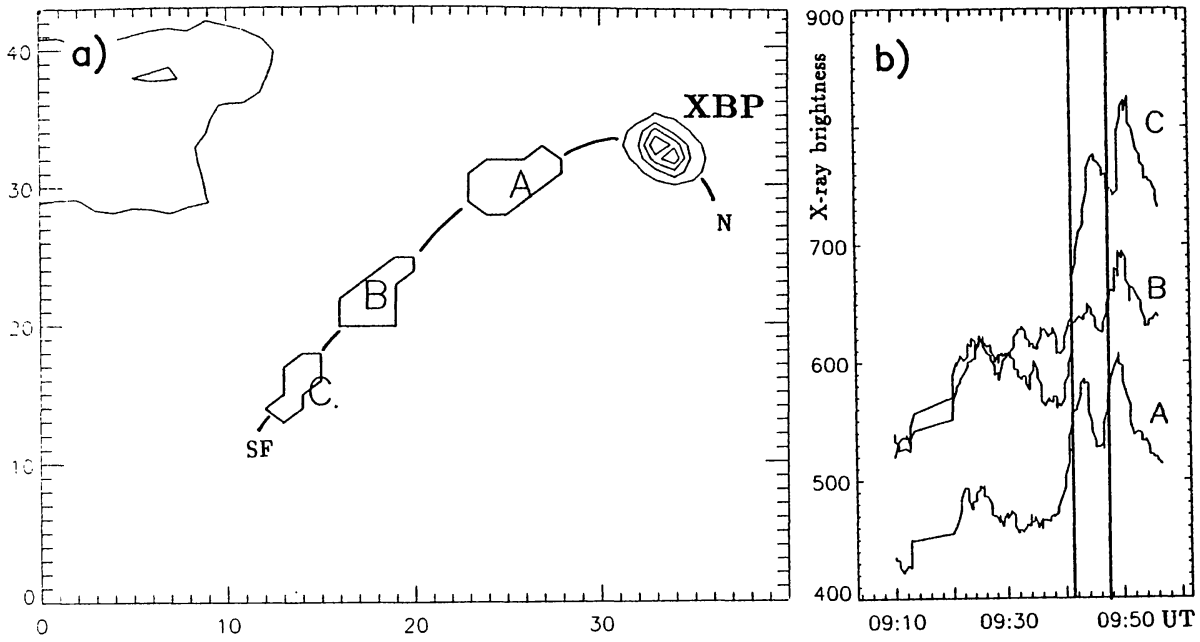

Figure 5. Time evolution of the X-ray brightness along the coronal loop FXL. (a) Isocontour maps showing the locations A, B, C along the loop. (b) Time evolution of X-ray brightness at the locations A, B, and C. The vertical lines indicate the time of two brightness peaks (flares) for the XBP (see Paper I). A time delay in the brightness at different positions along the FXL shows the propagation of energy from the XBP. The site of primary energy release is located where the AFS and PCL interact. The spatial scale of the contour plot is given in pixels (1 pixel $\approx$ 1.8 Mm) and the vertical scale of the light curves is data number s^{-1}.

length (L), and the delay function ($T = \int ds/B$, where the integration is performed along a magnetic field line). The first two functions have a jump discontinuity at separatrices, while the third one has a logarithmic one (Lau, 1993). These discontinuities are related to the presence of a magnetic null point in the corona. When no null point is present, D, L, and T take a standard continuous shape when plotted in the scale-length of the QSL thickness, as seen in Figures 4(a), 4(c), and 4(d); however, a steep change in the three functions is still present when they are analysed in the scale-length of the magnetogram resolution (Figure 4(b)). The conclusion arising from the variation of these three functions is the same as the one derived from N, as these steep changes occur in the same scale-length.

3.4. Discussion of the Reconnection Rate

As illustrated in Figure 6 and Table III of Paper I, at the time of P1 magnetogram the XBP brightness is increasing and between 08:04 and 14:34 UT on May 1, 11 XBP flares were observed with a peak intensity at 09:49 UT. At the time of H1, the XBP is fading though still visible and flares are again observed at 19:42 UT and at 20:27 UT. Following the gap in the *Yohkoh* observations, from 02:00 UT on May 2, a very low XBP brightness is observed. Flaring episodes superimposed on a gradual evolution, have also been observed in other cases (e.g., Strong *et al.*,

1992). What is the cause of the gradual brightness evolution and what leads to flares? Below, we propose a scenario, based on the above XBP observations and the present knowledge of 3D magnetic reconnection, in which both regimes are included.

Let us first analyse the gradual brightness evolution of the XBP. According to Priest and Démoulin (1995), when smooth boundary motions are imposed, reconnection occurs preferentialy along QSLs. The basic reason is that, at coronal heights, the field-line velocity is proportional to the value of the norm N (Equation (1)) at the photospheric level, so the coronal velocity may become very large in the QSLs. The consequence of this is that the field-line velocity greatly exceeds the possible plasma velocity; under these conditions, the field lines slip rapidly through the plasma and a component of the electric field appears along the magnetic field in the layer. Hence, magnetic reconnection is forced by boundary motions in the QSLs. Let us roughly test this scenario in the case of the XBP studied. With the velocity measured from observations for the new negative pore and the value of $N_{\max}$ computed at points O, P, and Q, we can calculate the field-line velocity (v_l) and compare it to the possible plasma velocity, whose upper bound is typically of the order of v_A,

$$v_A = 2.8 \times 10^6 B n^{-0.5} \quad (\mathrm{km\ s^{-1}})\,, \tag{2}$$

with the magnetic field magnitude (B) in G and n in $\mathrm{cm^{-3}}$. The values of $N_{\max}$ at points O, P, and Q are $\approx 10^4$, 4×10^5 and 70, respectively (see Figure 4); therefore, with the measured velocity of 0.2 km $\mathrm{s^{-1}}$, we obtain $v_l \approx 2 \times 10^3$ km $\mathrm{s^{-1}}$, 8×10^4 km $\mathrm{s^{-1}}$ and 14 km $\mathrm{s^{-1}}$ for P1, H1, and H2 magnetograms. We take $B \approx 50$ G for P1 and 100 G for H1 and H2 as an upper bound for the coronal field magnitude (see Figure 3) and $10^9\ \mathrm{cm^{-3}} \leq n \leq 10^{10}\ \mathrm{cm^{-3}}$ for an order of magnitude estimate (from the soft X-ray emission measure we find a density of $\approx 4 \times 10^9\ \mathrm{cm^{-3}}$ in the FXL and of $\approx 8 \times 10^9\ \mathrm{cm^{-3}}$ in the XBP). With these values, we find that $1.4 \times 10^3\ \mathrm{km\ s^{-1}} \leq v_A \leq 4.4 \times 10^3\ \mathrm{km\ s^{-1}}$ for P1 magnetogram and $3 \times 10^3\ \mathrm{km\ s^{-1}} \leq v_A \leq 9 \times 10^3\ \mathrm{km\ s^{-1}}$ for H1 and H2 magnetograms. These values are upper-bound estimates of the Alfvén velocity in the FXL because we use the magnetic intensity at the loop footpoint. Nevertheless they turn out to be of the order of v_l ($\approx 2 \times 10^3$ km $\mathrm{s^{-1}}$) for P1 magnetogram and much lower than v_l ($\approx 8 \times 10^4$ km $\mathrm{s^{-1}}$) for H1 magnetogram, while this is not so for H2 ($v_l \approx 14$ km $\mathrm{s^{-1}}$). Then quasi-steady magnetic reconnection can be forced by photospheric motions in the first two cases, giving the observed gradual brightness, while the evolution can be nearly ideal (without reconnection) in the last case, giving a low brightness as observed; the XBP has probably faded by the time of H2.

Next we consider the flaring episodes. When the evolution of the magnetic configuration can be considered to be quasi-static, Démoulin *et al.* (1996a) have shown that concentrated currents are naturally formed at QSLs by smooth photospheric

motions. This is so because the effect of photospheric displacements is augmented in these thin regions. Along the QSLs two neighbouring field lines are subjected to different photospheric motions since their opposite footpoints are separated by a great distance; therefore, electric currents are mainly created at the QSLs. For a smooth photospheric flow pattern, the current density is expected to be larger where the QSL is thinner. However, at the places where QSLs are too thin, say lower than a certain δ_{crit}, reconnection is initiated and the free magnetic energy is released (see above paragraph). At the places where $\delta > \delta_{\text{crit}}$, mainly electric current build-up is achieved until a threshold is reached; then there is a brusque release of magnetic energy giving the flaring episodes of the XBP. As discussed by Démoulin *et al.* (1996a), the kind of threshold reached in the solar atmosphere is not known; it can be a threshold on the current density (current-driven instability) or on the total twist in the magnetic field (ideal instability of the configuration). In the case of AR 7493 we cannot assert the existence of photospheric current concentrations, though we can imagine that the displacement of the new negative pore, with a velocity of 0.2 km s^{-1}, should induce such concentrated currents.

The temporal evolution of the energy release observed in this XBP leads to the conclusion that the XBP itself comes from magnetic reconnection forced by flux emergence. In the thinnest portion of QSLs reconnection can be steady, while in the other portions we have first a build up of electric currents (hence storage of magnetic energy) and then a local breakdown of the equilibrium leading to a small flare. To test this scenario further we need, on the theoretical side, to quantify the current build up as a function of the QSL thickness and the imposed flow pattern and, on the observational side, to measure the evolution of the electric currents, a challenge for the next generation of magnetographs. As a first step, it would be useful to investigate the degree of impulsivity in energy release of a set of magnetic regions as a function of the topological properties of the regions, in particular as a function of the thickness of QSLs.

3.5. Mechanism of Energy Transport along the Faint X-ray Loops

Brightness enhancements at the remote footpoints of the FXL were found in Paper I, suggesting that the system was heated by both fast particles (which travel along the loops in a few seconds) and a conduction front (540 km $s^{-1} \leq v \leq 850$ km s^{-1}). The evolution of the brightness, during the most active period of the XBP, is shown in Figure 5(b) at selected regions along the FXL (see Figure 5(a)); an average of the data on 5 time steps is used to increase the signal-over-noise ratio. Two intensity maxima are seen propagating along the loops. The times corresponding to these two maxima in the XBP light curve are shown for reference with vertical lines (see Paper I). Even though the statistics of the signal are low, the two peaks can be identified as they move along the FXL from the XBP towards footpoint SF. From the magnetic field extrapolation we can obtain the corresponding length of the field lines, which is 120 ± 10 Mm. Averaging the time delay measured between the XBP

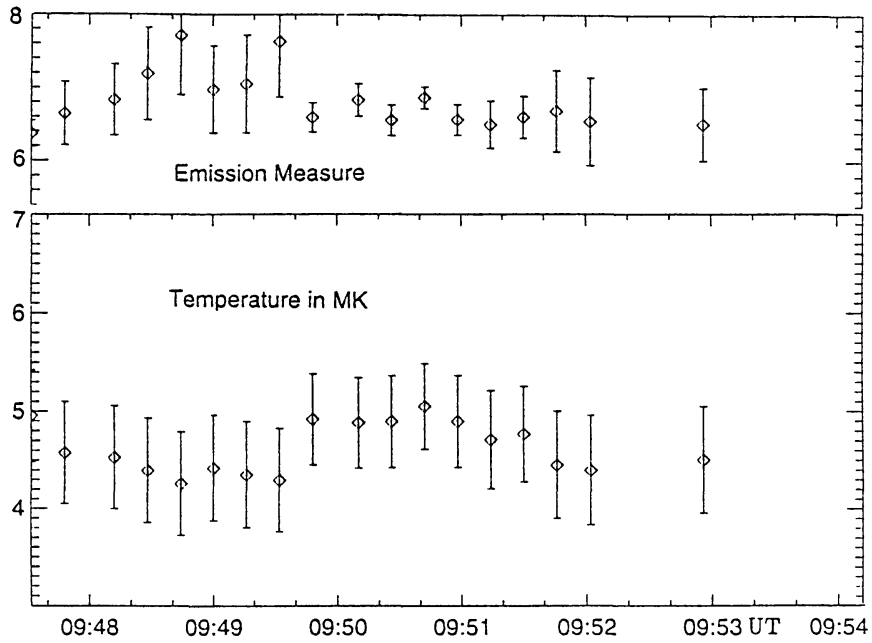

Figure 6. Temperature and emission measure evolution in the FXL, related to the largest XBP flare, at a point close to the footpoints of the FXL in SF. An increase (respectively, decrease) of the temperature (respectively, emission measure) is observed at ≈ 09:49:40 UT. The temperature is in units of 10^6 K and the emission measure in units of 10^{27} cm^{-5}.

maximum and the one in C for the two peaks, we obtain a time delay of 150 ± 20s. This implies a propagating velocity $v_p = 670 \pm 120$ km s^{-1}.

What is the mechanism which transports the energy from the reconnection region (near the XBP) to the footpoints of the FXL located in SF: accelerated particles, plasma waves, shock waves, or conduction fronts? The weak simultaneous increase in brightness at the XBP and at the footpoints of the FXL can be due to the energy deposited by fast particles accelerated at the reconnection region (see Paper I), but we still have to explain the observed time delay for the brightness propagation. From soft X-ray data (Figure 6) we estimate an average temperature $T \approx 4.5 \times 10^6$ K and a density $n \approx 3.8 \times 10^9$ cm^{-3} for the whole FXL; the last value coming from an average emission measure of $\approx 8 \times 10^{27}$ cm^{-5} considering the line-of-sight thickness of the loop to be approximately 3 pixels (1 pixel $\approx 1.8 \times 10^8$ cm).

First, let us consider plasma waves. They can be classified according to their phase velocity as slow, intermediate (the so-called Alfvén waves), and fast magnetoacoustic modes. For the latter two modes and the plasma parameters determined, the propagation speed is typically the Alfvén speed (v_A). For an order of magnitude estimate, taking a value of B between 10 G at the FXL top and 100 G at the FXL footpoints, we find that v_A is between 450 and 4500 km s^{-1}. Since we do not observe such a high velocity difference in the propagation of the brightness between the footpoints and the top of the FXL, but rather a nearly constant velocity (see Figure 5(b)), we believe that fast and intermediate modes can be ruled out. Moreover the same arguments used by Rust *et al.* (1985), concerning the direction

of propagation of fast modes that is orthogonal to the field, and those of Strong *et al.* (1992), concerning the difficulty of dissipating the energy carried by plasma waves, can be used to discard them. The velocity of the slow MHD mode is approximately the sound speed (c_s) in a plasma with a low β parameter, like that of the low corona. With the above T, $c_s = 0.152\sqrt{T}$ km s^{-1} $\approx$ 350 km s^{-1}; this value is twice as low as that needed to explain the observations. Therefore, no kind of plasma wave looks suitable for energy transport along the FXL.

Can a shock wave travelling faster than the sound speed explain the observations? According to Strong *et al.* (1992), the velocity of an adiabatically expanding plasma moving in a one-dimensional flow is

$$v_{\text{shock}} = 3\, c_s \left[1 - \left(\frac{p_e}{p_o}\right)^{1/5}\right] , \tag{3}$$

where p_e and p_o are respectively the pressure of the FXL and of the high-pressure plasma expanding along them. If p_e is negligible compared to p_o, the maximum v_{shock} is $3c_s$. For $v_{\text{shock}} \approx 2c_s$ as needed to explain the observations, $p_e/p_o \approx 4 \times 10^{-3}$. This last value is not supported by the X-ray data. As the brightness peak reaches the lowest portion of the FXL (at $\approx$ 09:49:40 UT in Figure 6), an increase of $\approx$ 10% in T is observed while the emission measure decreases in about the same amount. Because the magnetic pressure dominates over the gas pressure, it is unlikely that the loop expands laterally in a significant way, so the previous result implies a decrease of the density by $\approx$ 5%. This means that p_e is lower than p_o only by $\approx$ 5%. Using this result we obtain $v_{\text{shock}} \approx 5\% c_s$, a velocity much lower than the observed v_p. Therefore, we can also rule out transport by a shock wave along the FXL.

Another possible energy transport mechanism is a thermal conduction front. The velocity of the front is $v_{\text{cond}} = f v_e$, where v_e is the electron thermal velocity and f a coefficient that has a maximum value $\approx$ 0.4 in a limited heat flux (Campbell, 1984). With the value of T found above, v_{cond} has a maximum value of 3500 km s^{-1} which is well above the observed velocity. In order to fit the observations, we need $f \approx 0.08$, a value similar to that found by Rust *et al.* (1985) for flares (0.11). From Table I in Campbell (1984), this last value corresponds to a scalelength for the temperature gradient only 3 times larger than the mean free path of electrons and a heat flux reduced by about 20% from the classical heat flux ($\kappa T^{5/2} \nabla T$, where κ is the coefficient of thermal diffusivity). Then, we conclude that the observed brightness displacement is compatible with the existence of a flux-limited thermal front transporting the energy along the FXL. This is in agreement with the conclusions of Rust *et al.* (1985) and Bagalá *et al.* (1995) for flares. The range of possible velocities for thermal fronts is also compatible with the observed range (a few hundred to one thousand km s^{-1}) obtained by Strong *et al.* (1992).

4. Conclusion

Ground-based optical observations coordinated with those of *Yohkoh*/SXT of an old, disintegrating bipolar active region (NOAA 7493) provided a multiwavelength (magnetic field, Hα and X-ray) data base for the study of a flaring X-ray bright point (XBP) of about 16 hour lifetime (Figure 1). The XBP is related to the emergence of a minor bipole of about 10^{20} Mx. Rather than having a round shape, it was a loop-like feature linking the new negative polarity to an old positive polarity facular region. Other X-ray loops (FXL), much longer and fainter, are linked to the XBP (Figure 1). Extrapolating 4 maps of the observed photospheric magnetic field, we find field lines in good agreement with the observations both of the emerging flux (seen in Hα as an arch filament system) and the soft X-ray loops (XBP and FXL). The photospheric footpoints of these field lines are at both sides of the computed quasi-separatrix layers (QSLs), as expected from a 3D reconnection model. We show that the X-ray loops, XBP and FXL, were due to reconnection between the field lines corresponding to the new bipole and the pre-existing plage fields, and that this process was induced by the motion of one of the new pores towards the old plage with a velocity of 0.2 km s^{-1}. The difference in intensity between the two sets of X-ray loops (XBP and FXL) can easily be explained by the difference in volume between them; even if the same amount of energy is deposited in each set of loops, thermal conduction and particles would spread the energy in such a way that a lower brightness would be observed in the bigger loops.

In previous topological studies of AR magnetic fields, only the idea of separatrices has been applied (see references in the Introduction), which arose naturally from the direct extension of 2D reconnection models to observed configurations. Now it is known that coronal separatrices are present only in three cases: first, if a magnetic null point appears in the corona; second, if field lines are tangent to the boundary (i.e., photosphere); third, if the coronal magnetic field is modelled using localized sources and the topology determined considering the link between them. In general, the first two cases have not been found in flaring configurations (Démoulin, Hénoux, and Mandrini, 1994) nor in the XBP configuration described in this paper. The third case is a useful representation of the coronal magnetic field, separatrices computed with sources are closed surfaces and portions of them have been found to be related to flare and XBP brightenings (see, e.g., Mandrini *et al.*, 1991, for flares or Parnell *et al.*, 1994, for XBPs). With the new concept of QSLs we can go further in the understanding of observations. First the model of the coronal field is only limited by our ability to compute it using directly the observed photospheric magnetic field. Second the locations of QSLs are spatially more restrictive than those of separatrices, since QSLs are located only along a fraction of the separatrices determined when sources are used (see Démoulin *et al.*, 1996a). Finally QSLs have generally a finite thickness that is associated with the rate of reconnection, while computation of the topology using sources gives as a result separatrices that are infinitely thin (by definition).

Our results agree with those of Parnell *et al.* (1994) showing that at least some X-ray bright loops can be interpreted, using magnetic field-line computations, as being reconnected magnetic loops. In the present work we put forward the evidence. First, we use a direct extrapolation of the observed photospheric magnetic field rather than discrete magnetic sources. Second, we use a more sophisticated technique to compute the 'topology' of the magnetic field, using the knowledge gained from flare modelling with source and QSL methods. Third, we have had the opportunity to analyse the observed motion of the emerging flux during a half day. This motion is shown to be consistent with the evolution of the locations of X-ray loops. The evolution of the thickness of the QSL, associated with one of the emerging pores, allows us to explain the global evolution of the X-ray intensity: initially the thickness decreases and the brightness increases, while later on the thickness becomes too large to allow significant magnetic energy release. Finally we show how the energy propagates along the long reconnected loops (FXL) (the other reconnected loop, the XBP, is too short for any measurement). The energy is released where the emerging bipole (AFS) impacts against the pre-existing coronal loops (PCL). Then we conclude, in accordance with Paper I, that the energy transport along the FXL is due to both fast particles and conduction fronts; the presence of the latter is mostly evident in soft X-rays.

The observation of this XBP shows an example of magnetic reconnection forced by emergence and displacement of a new bipole in an old magnetic field region. Steady magnetic reconnection is probably induced in QSLs that are thin enough so that the field-line motions greatly exceed the possible plasma motions in the corona (see Priest and Démoulin, 1995). Superimposed on this global evolution of soft X-ray brightness, the XBP displays flaring episodes lasting for 1–10 min. It may be that the reconnection regime becomes bursty, but another likely interpretation is the following. In the places where QSLs are not thin enough to allow reconnection, concentrated electric currents are formed (see Démoulin *et al.*, 1996a); then as the current density increases, a threshold is reached, leading to a sudden energy release. We are not able to test this hypothesis, since it would require both much higher spatial resolution and sensitivity in the transverse field measurements. It will certainly be very exciting to combine magnetograms obtained with instruments of the new generation (like THEMIS) with coronal observations to learn in more detail how reconnection works in such complex 3D magnetic configurations. For this goal, the simplest magnetic configurations, where minor brightenings occur, will be the best canditates for the diagnosis.

Acknowledgements

P.D. and C.H.M. acknowledge financial support from the CONICET (Argentina) and CNRS (France) through their Argentina–France cooperative science program. C.H.M. is grateful for travel support to Fundación Antorchas (Argentina) and the

group at DASOP for making her feel at home during her stay there. LvDG's work was partially supported by the Hungarian Research Grant T17325 OTKA I/7. Mees Solar Observatory is supported by NASA through grant NAGW-1542. G.C. achnowledges support by the National Science Foundation under grant ATM-9303873.

References

Alissandrakis, C. E.: 1981, *Astron. Astrophys.* **100**, 197.
Bagalá, L. G., Mandrini, C. H., Rovira, M. G., Démoulin, P., and Hénoux, J. C.: 1995, *Solar Phys.* **161**, 103.
Bungey, T. N., Titov, V. S., and Priest, E. R.: 1996, *Astron Astrophys.* **308**, 233.
Campbell, P. M.: 1984, *Phys. Rev.* **30**, 365.
Démoulin, P., van Driel-Gesztelyi, L., Schmieder, B., Hénoux, J. C., Csepura, G., and Hagyard, M. J.: 1993, *Astron. Astrophys.* **271**, 292.
Démoulin, P., Hénoux, J. C., and Mandrini, C. H.: 1994, *Astron. Astrophys.* **285**, 1023.
Démoulin, P., Mandrini, C. H., Rovira, M. G., Hénoux, J. C., and Machado, M. E.: 1994, *Solar Phys.* **150**, 221.
Démoulin P., Hénoux J. C., Priest E. R., and Mandrini, C. H.: 1996a, *Astron. Astrophys.* **308**, 643.
Démoulin, P., Bagalá, L. G., Mandrini, C. H., Hénoux, J. C., and Rovira, M. G.: 1996b, *Astron. Astrophys.*, submitted.
Golub, L., Krieger, A. S., and Vaiana, G. S.: 1976, *Solar Phys.* **49**, 79.
Golub, L., Harvey, J. W., and Webb, D. F.: 1986, in A. I. Poland (ed.), *Coronal and Prominence Plasmas*, NASA CP-2442, p. 365.
Golub, L., Krieger, A. S., Harvey, J. W., and Vaiana, G. S.: 1977, *Solar Phys.* **53**, 111.
Golub, L., Krieger, A. S., Silk, J. K., Timothy, A. F., and Vaiana, G. S.: 1974, *Astrophys J.* **189**, L93.
Gorbachev, V. S. and Somov, B. V.: 1988, *Solar Phys.* **117**, 77.
Gorbachev, V. S. and Somov, B. V.: 1989, *Soviet Astron.* **33**, 1, 57.
Harvey, K. L.: 1993, Ph.D. Thesis, University of Utrecht, The Netherlands.
Harvey, K. L., Nitta, N., Strong, K. T., and Tsuneta, S.: 1994, in Y. Uchida, T. Watanabe, K. Skibata, and H. S. Hudson (eds.), *X-ray Solar Physics from Yohkoh*, Frontiers Science Series, No. 10, p. 21.
Kundu, M. R., Strong, K. T., Pick, M., Harvey, K. L., Kane, S. R., White, S. M. and Hudson, H. S.: 1994, in S. Enome and T. Hirayama (eds.), *Proc. of Kofu Symposium*, NRO Report No. 360, p. 343.
Lau, Y. T.: 1993, *Solar Phys.* **148**, 301.
Lau, Y. T. and Finn, J. M.: 1990, *Astrophys. J.* **350**, 672.
Mandrini, C. H., Démoulin, P., Hénoux, J. C., and Machado, M. E.: 1991, *Astron. Astrophys.* **250**, 541.
Mandrini, C. H., Rovira, M. G., Démoulin, P., Hénoux, J. C., Machado, M. E., and Wilkinson, L. K.: 1993, *Astron. Astrophys.* **272**, 609.
Mandrini, C. H., Démoulin, P., Rovira, M. G., de la Beaujardière, J. F., and Hénoux, J. C.: 1995, *Astron. Astrophys.* **303**, 927.
Martin, S. F., Livi, S. H. B., Wang, J., and Shi, Z.: 1985, in M. J. Hagyard (ed.), *Measurements of Solar Vector Magnetic Fields*, NASA CP-2374, p. 403.
Mickey, D. L.: 1985, *Solar Phys.* **97**, 223.
Nolte, J. T., Solodyna, C. V., and Gerassimenko, M.: 1979, *Solar Phys.* **63**, 113.
Parnell, C. E., Priest, E. R., and Golub, L.: 1994, *Solar Phys.* **151**, 57.
Priest, E. R. and Démoulin, P.: 1995, *J. Geophys. Res.* **100**, A12, 23443.
Priest, E. R. and Forbes, T. G.: 1992, *J. Geophys. Res.* **97**, A2, 1521.
Priest, E. R. and Titov, V. S.: 1996, *Phil. Trans. Roy. Soc. London* **355**, in press.
Rust, D. M., Simnett, G. M., and Smith, D. F.: 1985, *Astrophys. J.* **288**, 401.
Schindler, K., Hesse, M., and Birn, J.: 1988, *J. Geophys. Res.* **93**, 5547.

Staude, J., Hofmann, A., and Bachmann, G.: 1991, in L. November (ed.), *Solar Polarimetry*, Sunspot, New Mexico, p. 49.

Strong, K. T., Harvey, K. L., Hirayama, T., Nitta, N., Shimizu, T., and Tsuneta, S.: 1992, *Publ. Astron. Soc. Japan* **44**, L161.

Tsuneta, S., Acton, L., Bruner, M., Lemen, J., Brown, W., Caravalho, R., Catura, R., Freeland, S., Jurcevich, B., Morrison, M., Ogawara, Y., Hirayama, T., and Owens, J.: 1991, *Solar Phys.* **136**, 37.

van Driel-Gesztelyi, L., Hofmann, A., Démoulin, P., Schmieder, B., and Csepura, G.: 1994, *Solar Phys.* **149**, 309.

van Driel-Gesztelyi, L., Schmieder, B., Cauzzi, G., Mein, N., Hofmann, A., Nitta, N., Kurokawa, H., Mein, P., and Staiger, J.: 1996, *Solar Phys.* **163**, 145 (Paper I).

van Speybroek, L. P., Krieger, A. S., and Vaiana, G. S.: 1970, *Nature* **227**, 818.

Webb, D. F., Martin S. F., Moses, D., and Harvey, J. W.: 1993, *Solar Phys.* **144**, 15.